



Validated shipping noise maps of the Northeast Atlantic

Adrian Farcas^{a,*}, Claire F. Powell^a, Kate L. Brookes^b, Nathan D. Merchant^a

^a Centre for Environment, Fisheries & Aquaculture Science (Cefas), Lowestoft, Suffolk, UK

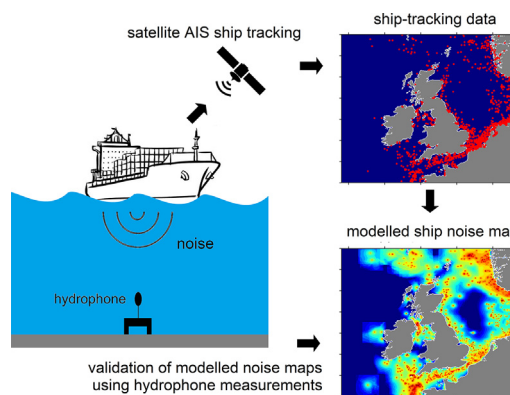
^b Marine Scotland Science, Aberdeen, Aberdeenshire, UK



HIGHLIGHTS

- Shipping noise is globally pervasive and impacts marine species which rely on sound.
- To manage ship noise pollution effectively, ground-truthed noise maps are needed.
- We present the first such validated maps of shipping noise at large scale.
- Predictions were within ± 3 dB for 93% of measurements in the range 125 Hz–5 kHz.
- Our results give confidence that ship noise mapping can be used to guide management.

GRAPHICAL ABSTRACT



ARTICLE INFO

Article history:

Received 28 February 2020

Received in revised form 22 April 2020

Accepted 16 May 2020

Available online 19 May 2020

Editor: Dr. Damia Barcelo

Keywords:

Noise pollution

Shipping

Anthropogenic

Marine spatial planning

Marine policy

ABSTRACT

Underwater noise pollution from shipping is globally pervasive and has a range of adverse impacts on species which depend on sound, including marine mammals, sea turtles, fish, and many invertebrates. International bodies including United Nations agencies, the Arctic Council, and the European Union are beginning to address the issue at the policy level, but better evidence is needed to map levels of underwater noise pollution and the potential benefits of management measures such as ship-quieting regulations. Crucially, corroboration of noise maps with field measurements is presently lacking, which undermines confidence in their application to policymaking. We construct a computational model of underwater noise levels in the Northeast Atlantic using Automatic Identification System (AIS) ship-tracking data, wind speed data, and other environmental parameters, and validate this model against field measurements at 4 sites in the North Sea. Overall, model predictions of the median sound level were within ± 3 dB for 93% of the field measurements for one-third octave frequency bands in the range 125 Hz–5 kHz. Areas with median noise levels exceeding 120 dB re 1 μ Pa and 20 dB above modelled natural background sound were predicted to occur in the Dover Strait, the Norwegian trench, near to several major ports, and around offshore infrastructure sites in the North Sea. To our knowledge, this is the first study to quantitatively validate large-scale modelled noise maps with field measurements at multiple sites. Further validation will increase confidence in deeper waters and during winter months. Our results highlight areas where anthropogenic pressure from shipping noise is greatest and will inform the management of shipping noise in the Northeast Atlantic. The good agreement between measurements and model gives confidence that models of shipping noise can be used to inform future policy and management decisions to address shipping noise pollution.

© 2020 The Authors. Published by Elsevier B.V. This is an open access article under the Open Government License (OGL) (<http://www.nationalarchives.gov.uk/doc/open-government-licence/version/3/>).

* Corresponding author.

E-mail address: adrian.farcas@cefas.co.uk (A. Farcas).

Editor: Dr. Damia Barcelo

1. Introduction

Shipping is the primary vehicle of global trade (~80% by volume; UNCTAD, 2017), and has risen significantly as a consequence of globalisation, with seaborne trade growing fourfold by tonnage since 1970 (UNCTAD, 2017). Measurements from the Northeast Pacific indicate that this rise in global shipping has led to a correlated rise in underwater noise pollution (Frisk, 2012), with noise levels in that area increasing by up to 10 dB between the 1960s and the 1990s at low (<300 Hz) frequencies (Andrew et al., 2002). While such long-term records are lacking elsewhere (including in the Northeast Atlantic), it is expected that growth in motorised shipping since its advent in the 19th century has led to corresponding rises in underwater noise pollution in other parts of the global ocean.

Exposure to underwater noise pollution from shipping is known to cause a range of detrimental effects in marine mammals, fish, and invertebrates, including heightened physiological stress levels (Rolland et al., 2012; Debusschere et al., 2016; Wysocki et al., 2006), disruption of behaviour (Blair et al., 2016; Nowacek et al., 2007; Weilgart, 2018; Wisniewska et al., 2018), and masking of acoustic communication (Parks et al., 2007; Putland et al., 2018; Stanley et al., 2017).

This scientific evidence of harm to marine life and the rising levels of shipping noise pollution have led to growing recognition of the issue at the policy level. Intergovernmental bodies including the United Nations (UN, 2018), the European Union (European Commission, 2017), and the Arctic Council (PAME, 2019) have enacted legislation or begun initiatives to address noise pollution from shipping (and other human activities). Importantly, the International Maritime Organisation (IMO) has also issued advisory guidance on quieting individual ships (IMO, 2014). Some jurisdictions have now enacted ship speed reduction measures to reduce noise in the seasonal habitat of endangered species (Joy et al., 2019).

To assess the risk that shipping noise pollution poses to marine life and to evaluate the efficacy of management measures to reduce this risk, reliable predictions of the levels and distribution of shipping noise pollution are needed (Cefas, 2015). Modelled large-scale maps of shipping noise have been produced for several regions (e.g. Aulanier et al., 2017; Erbe et al., 2012; Sertlek et al., 2019). However, these have yet to be validated using in situ field measurements, which limits confidence in their applicability to management.

Some limited validation has been done for single measurement locations, e.g. both Bassett et al. (2012) and Aulanier et al. (2016) compared shipping noise maps to measurements at a single site, although the ship noise levels used in the models were themselves derived from the same measurements (i.e. not a generic ship noise model), which limits the applicability of the results to other sites or ship source models. Joy et al. (2019) provided a comparison of measurements with model at a single site, but only a night-time subset of data were presented. In the grey literature, one study has tested a generic ship source model against single-site measurements (MacGillivray et al., 2014) but the level of agreement was not well quantified, and another single-site study showed poor agreement (AQUO, 2015). Consequently, the ability of these previous models to make valid predictions at any site other than the measurement location remains unproven. Until this knowledge gap is addressed, decision makers can have little confidence in the use of ship noise mapping for marine spatial planning.

The aim of this study was to carry out a multi-site validation of a large-scale shipping noise map constructed using a generic shipping noise model. We present monthly and annual shipping noise maps of the Northeast Atlantic for 2017, validated against field measurements at four sites in the North Sea. The agreement of the model with measurements is quantified, enabling an assessment of the confidence with which shipping noise models can predict in situ noise levels. These results will inform the development of ship noise management

in this region, and help to guide ongoing efforts to improve the management of noise pollution from shipping in other regions.

2. Methods

Ocean noise maps are produced using data on noise sources (acoustic source spectrum level and location at each time increment) and the sound propagation properties of the environment. At low frequencies (<1 kHz), ocean noise is typically dominated by shipping and wind (Wenz, 1962). To produce maps of this sound field, these components are modelled separately [Fig. 1(a-d)] and then combined [Fig. 1(e-f)]. The predictions can then be validated against field measurements.

2.1. Source modelling

Several models are available to estimate ship source levels, including models which characterise noise from individual vessels according to ship speed and length (Breeding Jr et al., 1996; Ross, 1976). However, subsequent measurements have not supported these predictions (McKenna et al., 2013; Simard et al., 2016; Wales and Heitmeyer, 2002). An alternative to individual-based models is an ensemble ship source model, which predicts the average spectral source level of the entire fleet. Such an ensemble model, developed by Wales and Heitmeyer (2002), has subsequently been further corroborated with field measurements in the North Sea (Jansen and De Jong, 2017), including an extrapolation from the original maximum frequency of 1.2 kHz up to 16 kHz. This model was selected for the ship source levels, for third-octave bands centred between 63 Hz and 5 kHz.

Vessel positions were derived from satellite Automatic Identification System (AIS) data for the North East Atlantic area (48°N - 62°N latitude and 16°W - 9°E) for 2017. The dataset contained ~120,000 unique vessels, with positional data transmitted at short but irregular intervals (~5–30 min). These data were interpolated to 10-min resolution, yielding 52,560 vessel position frames for 2017. Stationary vessels and vessels with apparent speeds exceeding 15 m s⁻¹ (~29 knots) were excluded from the dataset.

Sound pressure levels of wind-generated noise were modelled based on Reeder et al. (2011). Wind speed data were sourced from the ECMWF ERA-Interim global atmospheric reanalysis (ECMWF, 2019), with a spatial resolution of 80 km and temporal resolution of 6 h, and interpolated to the resolution of the model grid (5 or 1.3 km, and 10 min). The Reeder et al. (2011) wind noise model is based on a dataset from a topographically isolated basin in the Atlantic Ocean which is believed to be free from significant levels of shipping noise.

2.2. Propagation modelling

Sound propagation was modelled using the energy-flux method (Weston, 1971), a computationally efficient range-dependent model which depends on bathymetry, sound speed, seabed reflectivity and acoustic frequency. Use of other models (e.g. parabolic equation) was investigated, but found to be computationally infeasible due to the large number of source/receiver transects required to produce the maps, and agreement between the chosen model and the depth-averaged predictions of a parabolic equation method (RAM; Collins, 1993) was found to be good, although both model predictions can be strongly dependent on the parametrisation of the seabed and thus require optimisation of the seabed acoustic properties (Farcas et al., 2016). Bathymetry data was extracted from EMODNET with 7.5" resolution, temperature and salinity data from the Copernicus Atlantic European North West Shelf Ocean Physics Analysis and Forecast product (0.016° × 0.016°, 33 depth levels, daily mean values) (Copernicus, 2019). Seabed acoustic properties were derived from the Hamilton model (Hamilton, 1987) using EMODNET seabed sediment data.

To improve computational efficiency, model domains can be gridded at different spatial resolutions to reflect spatial differences in model

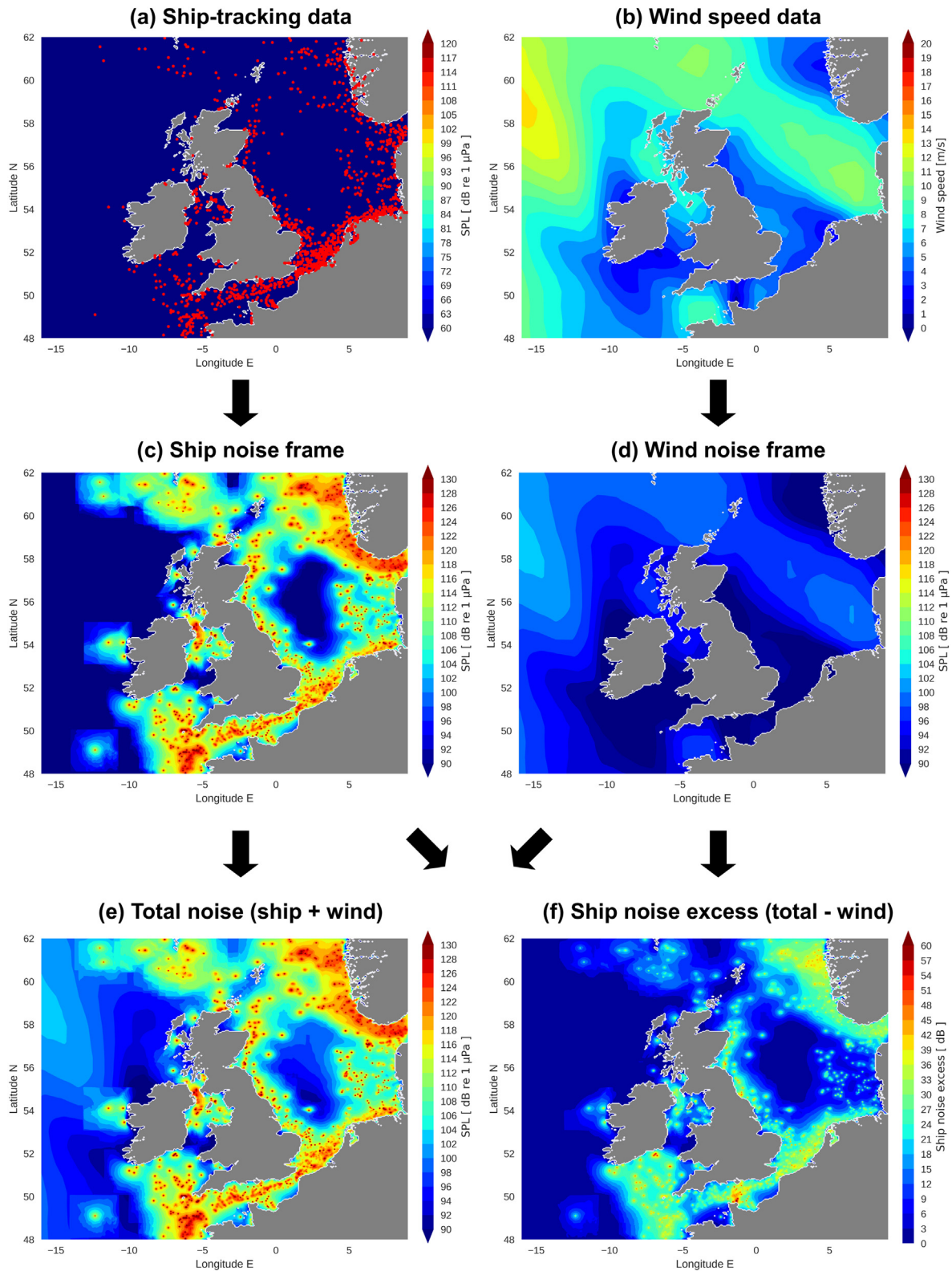


Fig. 1. Construction of total noise and ship noise excess maps. (a) sAIS ship-tracking data frame; (b) Wind speed data frame; (c) Ship noise frame corresponding to (a); (d) Wind noise frame corresponding to (b); (e) Total noise frame, sum of (c) and (d); (f) Excess level of ship noise above wind, (e) minus (d). Such frames were computed at 10-min intervals for calendar year 2017.

uncertainty (Trigg et al., 2018). The shipping noise model used spatial grids at two resolutions: a lower resolution grid with latitude-longitude spacing of 3' x 5' (approximately 5 x 5 km) for coverage of the entire domain, as well as a high-resolution grid of 0.75' x 1.25' (approximately 1.3 x 1.3 km) for selective coverage of smaller areas near

the coast and in areas of high shipping density, since this significantly improved accuracy at relatively low computational cost (see Supplementary Material for further details).

To improve computational efficiency, the bathymetry-dependent component of propagation loss was pre-computed and stored for each

spatial node of the computational grid, up to a range of 100 km. The actual values of the propagation loss also depend on the water column properties, which are both time- and frequency-dependent. These were calculated subsequently when the shipping sources were integrated into the model (see below).

2.3. Integration of propagation and source modelling components

Each vessel positional frame (Fig. 1a) was combined with the ship source model and applied to the propagation loss matrix for the corresponding month's water column properties, yielding an instantaneous map of the ship noise layer (Fig. 1c). The wind noise layer (Fig. 1d) computed from wind speed data (Fig. 1b) was then either added to the ship noise layer to produce a prediction of the total noise field (Fig. 1e) or subtracted from the total noise layer to produce a prediction of the excess level of the ship noise above wind (Fig. 1f; see Section 2.4 for details of this calculation). These frames were computed at 10-min intervals (yielding 52,560 frames for the year) for each one-third octave frequency band centred in the interval 63 Hz–5 kHz, and then analysed statistically to determine the median and P90 (90th percentile) statistics for each month and for the year overall. These metrics were chosen since percentiles of sound levels are more robust than the average (RMS level), which is skewed by unrepresentative high-amplitude events (Merchant et al., 2016). The median gives an indication of centroid levels, while P90 is more strongly influenced by transient events (Mennitt et al., 2014). In the Northeast Atlantic, where there is a high prevalence of shipping traffic, we postulate that monthly P90 will generally be dominated by shipping noise rather than to biological sources at the acoustic frequencies modelled.

2.4. Calculation of the broadband ship noise excess

The broadband ship noise excess was calculated by integrating the exceedance of total noise (shipping noise plus wind noise) above wind noise in each of the modelled 1/3-octave frequency bands, and then applying a correction scaled to the spectral width of the noise, which adjusts the minimum value of the broadband excess to zero if

no shipping noise is present at any frequency (Eq. (1)). This correction is needed since the minimum value of the ship noise excess would otherwise exceed zero and would scale with the frequency range over which it is calculated. The broadband ship noise excess, SPL_{excess} , is then given by

$$SPL_{excess} = \left[\sum_{i=1}^{i=N} (SPL_{total,i} - SPL_{wind,i}) \right] - 10 \log_{10} N \quad (1)$$

where N is the number of 1/3-octave frequency bands, $SPL_{total,i}$ is the total modelled sound pressure level from shipping and wind in the i th frequency band, and $SPL_{wind,i}$ is the modelled sound pressure level of wind only in the i th frequency band.

2.5. Validation

The model predictions were ground-truthed and optimised using concurrent field measurements from four monitoring stations off the east coast of Scotland, deployed as part of the Marine Scotland East Coast Marine Mammal Acoustic Study (ECOMMAS). Recordings were made using seafloor-mounted autonomous acoustic recorders (Wildlife Acoustics SM2M) between April and August 2017, sampling at 96 kHz on a duty cycle of 10 min on, 10 min off. The frequency dependence of the modelled seabed bottom loss parameter was calibrated using these measurements, yielding a correction factor at each frequency. This correction was applied uniformly throughout the model domain. Further technical details on the validation procedure and field deployments are provided in the Supplementary Material.

3. Results

3.1. Validation and calibration of shipping noise model

The validation of the model with measurements was carried out using monthly statistics of noise levels in each frequency band (Fig. 2). The initial parametrisation of the propagation loss model used standard

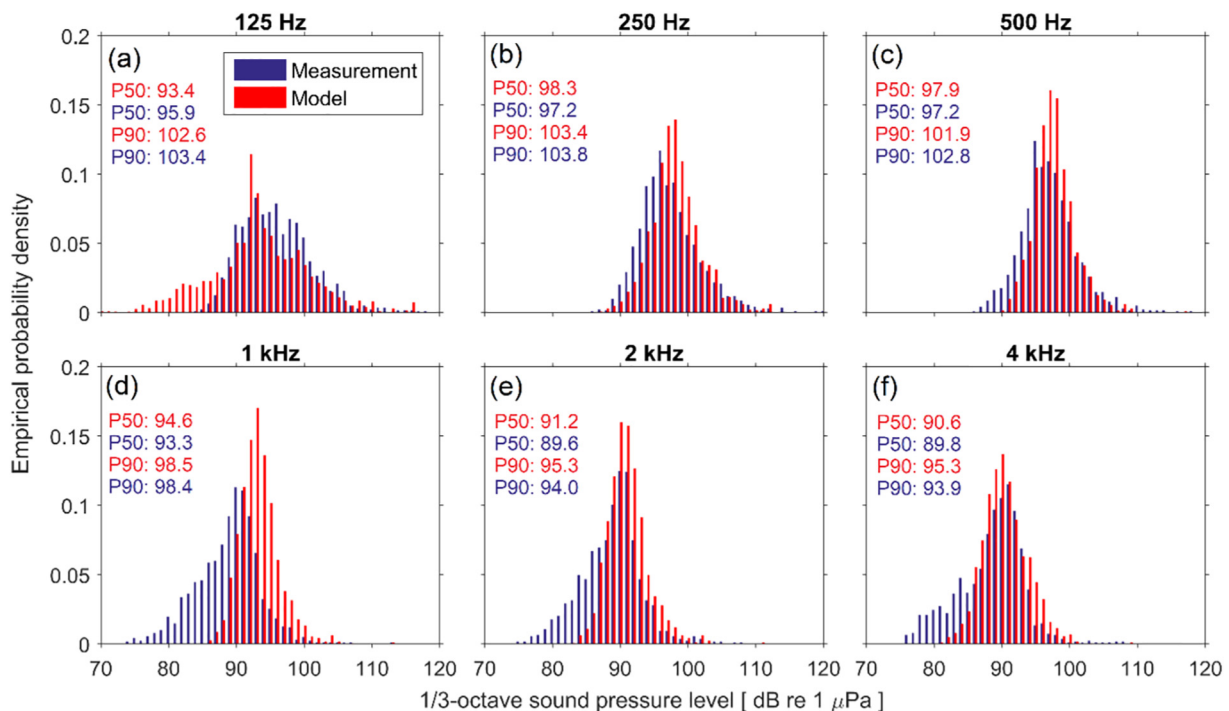


Fig. 2. Example comparison of modelled and measured noise levels at monitoring site 3 (56.257894° N, 2.499312° E) during April 2017 for six frequencies: (a) 125 Hz (b) 250 Hz (c) 500 Hz (d) 1 kHz (e) 2 kHz (f) 4 kHz. Modelled and measured P50 and P90 values are given in units of dB re 1 μPa.

literature values for the acoustic properties of the water column attenuation (Thorp, 1967), and seabed sediments (speed of sound: 1650 m s^{-1} ; density: 1.9 g cm^{-3} ; attenuation: $0.8 \text{ dB/wavelength}$) taken as representative of a sandy seabed (Jensen et al., 2011). This model gave good agreement (RMS error $< 3 \text{ dB}$) for the frequency bands in the range 315 Hz – 3.15 kHz (see Fig. S2), but produced significant discrepancies from the observed noise levels in the lower frequency bands between 63 Hz and 250 Hz , with only $\sim 50\%$ of monthly predictions being within $\pm 3 \text{ dB}$ of the measurements, for both median (P50) and the P90 statistics. These low-frequency errors were likely due to the strong dependence of low-frequency propagation loss in shallow-water waveguides on the acoustic properties of the seabed. For the water depths involved (typically tens of metres), the acoustic propagation regime over tens of kilometres will generally have progressed beyond the multi-mode region (where propagation loss depends more on bathymetry) and into single mode propagation, where the influence of seabed properties is paramount. These sediment attenuation properties can display a non-linear relationship with frequency (Farcas et al., 2016).

In the energy-flux model used, the seabed properties (sound speed, density and attenuation) are incorporated into a single model parameter, the seabed bottom loss (Weston, 1971). To improve the accuracy of model predictions across the frequency bands, we performed a

calibration of the seabed bottom loss by introducing a unique (i.e. applicable at all locations) frequency-dependent correction factor (see Supplementary Material for details). After this optimisation, the accuracy of model predictions (within $\pm 3 \text{ dB}$ of the observations) increased to 82% for P50 and 74% for P90, across all frequency bands, and to 93% for P50 and 78% for P90 across the 125 Hz – 5 kHz interval (excluding 1.25 kHz due to measurement error, see Supplementary Material). The mean errors were also $< 3 \text{ dB}$ in this frequency range. This improved seabed bottom loss model was selected for the final outputs shown below.

3.2. Broadband total noise and ship noise excess

Noise maps were produced for the extent of the available sAIS data for 2017 in the Northeast Atlantic. The annual median broadband (63 – 4000 Hz) noise level (P50; Fig. 3a) exceeded $120 \text{ dB re } 1 \mu\text{Pa}$ in parts of the English Channel and Norwegian Trench, and in localised areas of high shipping density around major ports (e.g. Aberdeen, Cork, Hamburg, Rotterdam), offshore installations in the northern North Sea, and at the confluence of shipping lanes and in narrow shipping channels (Fig. 3c). The P90 metric showed that much larger areas in these regions had broadband noise levels exceeding $120 \text{ dB re } 1 \mu\text{Pa}$ for 10% of the year (Fig. 3c). While this study does not attempt a risk assessment for different species in the region, a level of $120 \text{ dB re } 1 \mu\text{Pa}$

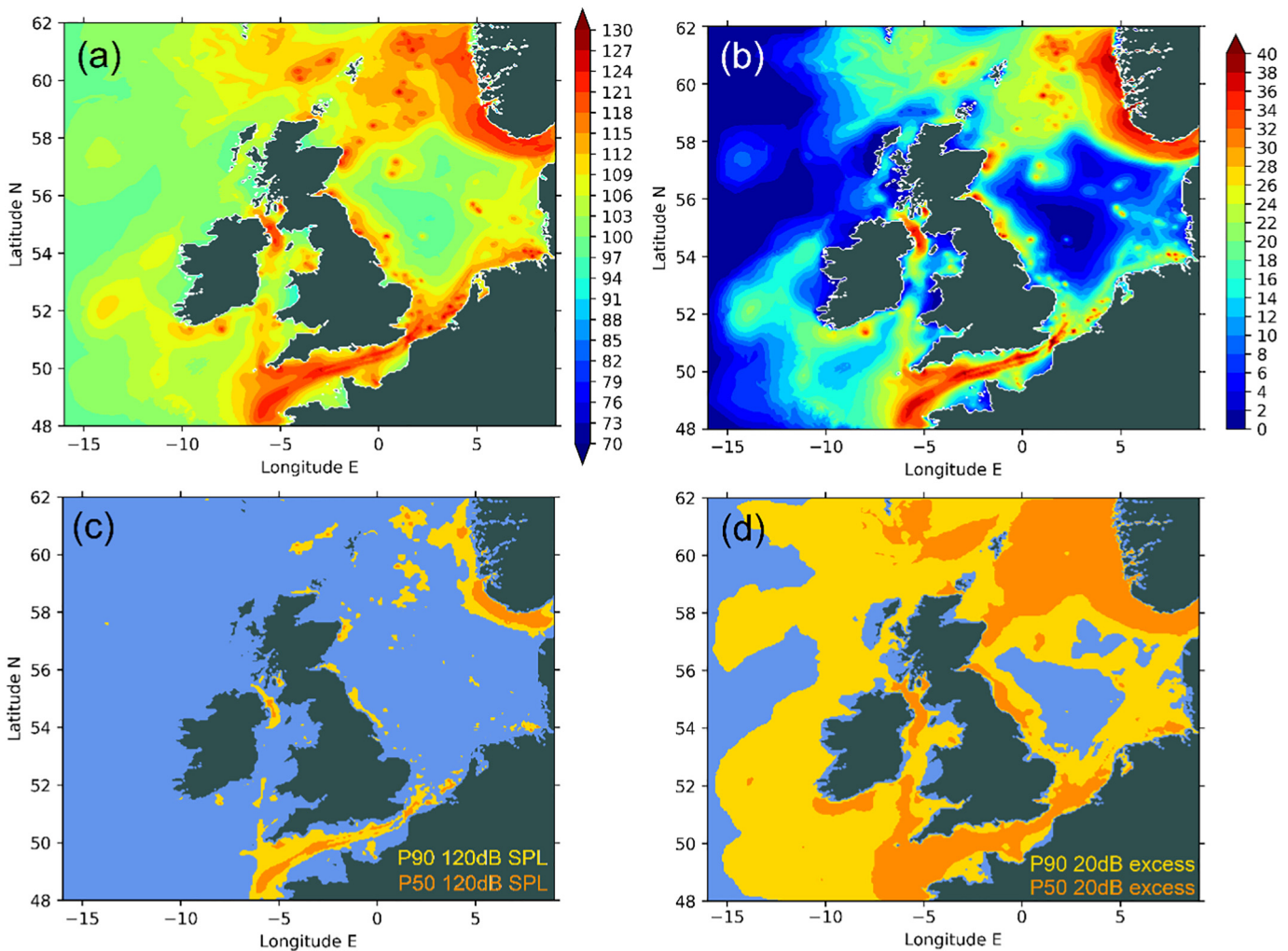


Fig. 3. Broadband (63 – 4000 Hz) total noise and ship noise excess maps for 2017 (a) Annual P50 total noise; colour scale shows sound pressure level in units of $\text{dB re } 1 \mu\text{Pa}$; (b) annual P50 ship noise excess; colour scale shows ship noise excess in units of dB ; (c) areas above $120 \text{ dB re } 1 \mu\text{Pa}$ broadband SPL for 50% of the year (P50) and 10% of the year (P90); (d) areas with ship noise excess above 20 dB for 50% of the year (P50) and 10% of the year (P90).

was considered a useful threshold since many studies have observed behavioural responses to noise in marine mammals at or above this level (Richardson et al., 1995; Richardson and Würsig, 1997) and it has been used as a threshold for disturbance to cetaceans in ship noise exposure assessments (e.g. Hatch et al., 2012; McQuinn et al., 2011).

The annual median ship noise excess (Fig. 3b) surpassed 20 dB in similar locations to the 120 dB re 1 μ Pa broadband threshold (Fig. 3c; Fig. 3d), albeit over much larger areas, and the P90 of this metric extended across large swathes of the domain, with only parts of the North Sea and deep-water Atlantic unaffected. These maps subtract the wind noise from the total noise level predicted for shipping and wind (see Fig. 1).

3.3. Frequency variability of ship noise excess

Noise from shipping and wind varies with frequency, according to both the frequency characteristics of the sources and the frequency dependence of underwater sound propagation. To examine frequency variation in ship noise excess, noise maps at a range of one-third-octave centre frequencies were produced (Fig. 4). They demonstrate an overall decrease in ship noise exceedance as frequency increases from 63 Hz to 4 kHz (Fig. 4). For reference, under the simplifying assumption of sound propagation via spherical spreading, a ship noise excess of 20 dB at a particular frequency corresponds to a 10-fold reduction in communication range at that frequency, and 40 dB corresponds to a 100-fold reduction (see Hermanssen et al., 2014; Möhl, 1981).

3.4. Temporal variability in ship noise excess

To assess seasonal variability, broadband ship noise excess maps were produced for selected months of data (Fig. 5). The maps demonstrate a summer peak in ship noise excess levels, with the highest levels in May and July (Fig. 5c, Fig. 5d) and the lowest levels in January and November (Fig. 5a, Fig. 5f).

4. Discussion

4.1. Significance of the results

The final noise model produced predictions of the median sound level which were within ± 3 dB in the frequency range 125 Hz–5 kHz for 93% of the field measurements (excluding 1.25 kHz band due to measurement error, see Supplementary Material), and had mean errors of < 3 dB in this frequency range (Table 1; Supplementary Material). This is a highly significant result since, to our knowledge, this is the first study to demonstrate and quantify the validity of ship noise mapping predictions with in situ measurements at multiple sites. The extent of agreement gives confidence that the model predictions are applicable to environments similar to where the field measurements were taken. Further validation in other environments (e.g. further offshore and in deeper/oceanic waters) would give further confidence in the model predictions throughout the domain modelled.

Comparison of an sAIS map (Fig. 1a) with the corresponding predictions of underwater noise (Fig. 1c) illustrates how noise levels differ from the shipping distribution based on the local acoustic propagation characteristics, particularly at low frequencies (Fig. 4). In the North Sea, predicted noise levels were generally lower in the southern North Sea than would be expected based solely on the sAIS shipping data, and higher in the northern part. This is due to the shallower bathymetry in the southern North Sea, which causes sound to reflect off the seabed more often, increasing the amount of acoustic energy lost as sound waves propagate. As frequency increases, propagation loss due to absorption in the water column also increases, meaning high frequency sound does not propagate as far as low frequency sound. Consequently, the shipping noise maps at higher frequencies more closely resemble the shipping distribution than those at lower frequencies [e.g. compare Fig. 4a and Fig. 4f to Fig. 1a], since the effect of bathymetry on acoustic propagation is less pronounced. These differences highlight why it is necessary to carry out acoustic modelling to inform management of ship noise pollution, since the results do not necessarily correspond to what might be expected based solely on the shipping distribution.

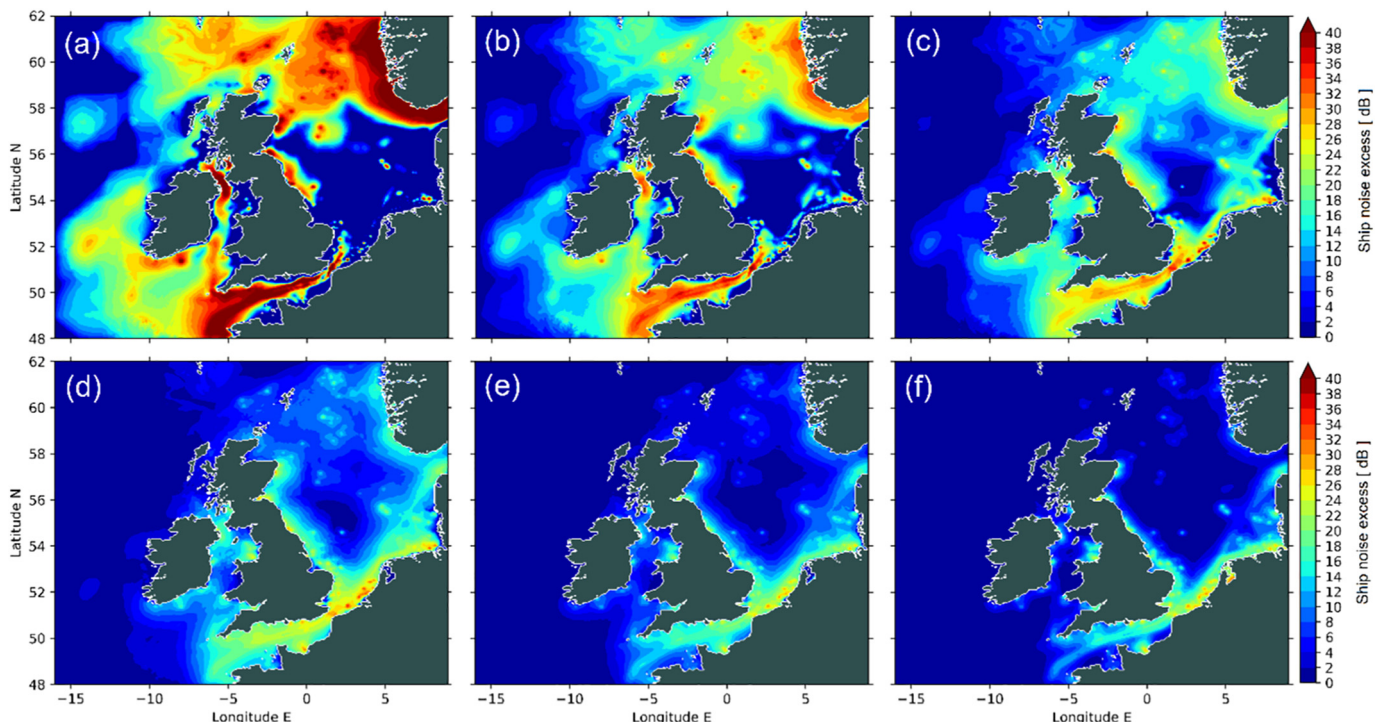


Fig. 4. Annual median ship noise excess (ship noise levels above wind) modelled at various frequencies: (a) 63 Hz (b) 125 Hz (c) 250 Hz (d) 500 Hz (e) 1 kHz (f) 4 kHz.

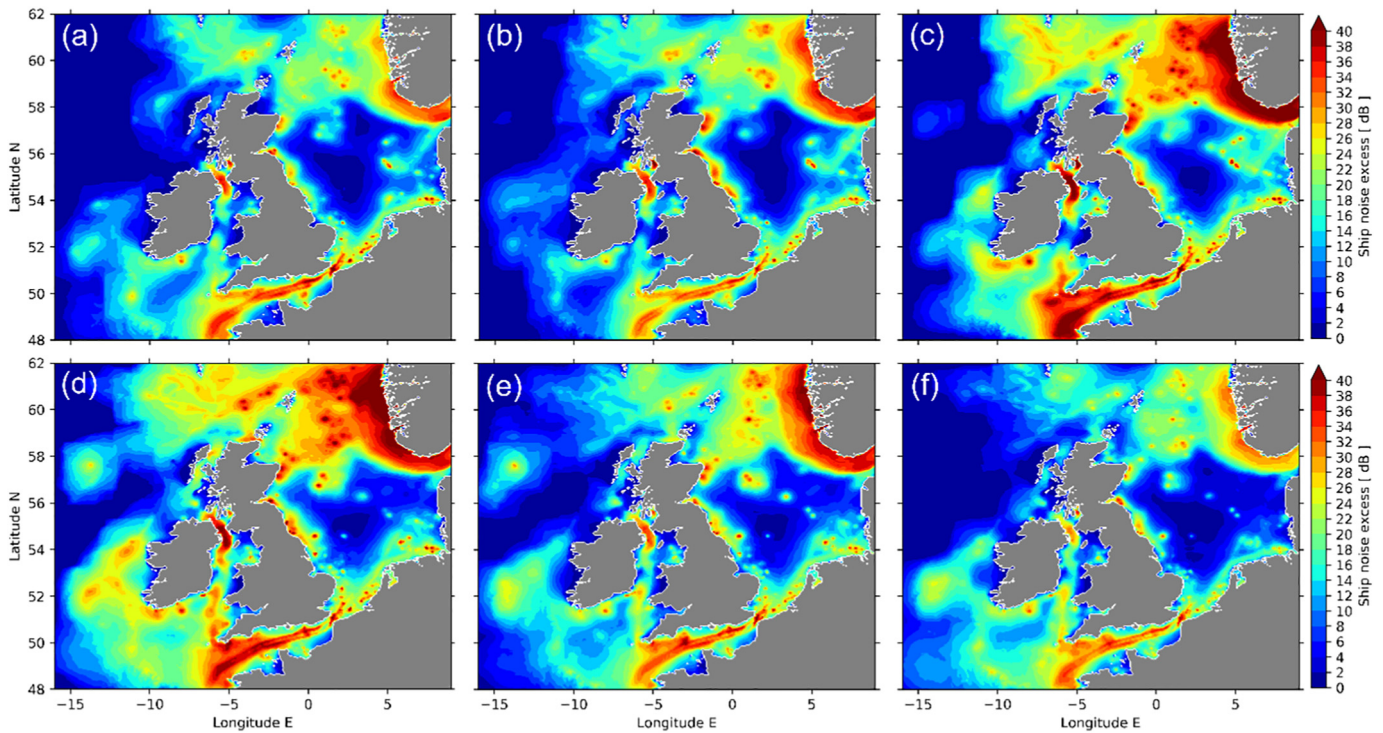


Fig. 5. Median broadband ship noise excess (ship noise levels above wind) for selected months in 2017. (a) January (b) March (c) May (d) July (e) September (f) November.

The highest noise levels predicted, both overall and as the exceedance above wind noise, were in the English Channel and along the UK east coast, particularly off the coasts of East Anglia, Humberside and Tyneside, and Aberdeen (Fig. 3a). High noise levels were also predicted in the northern North Sea, and the clustering of hotspots (Fig. 3a) suggests this is linked to oil and gas infrastructure. As noted above, the deeper waters in the northern North Sea allow the noise from this activity to propagate further than in the southern North Sea.

The maps of ship noise exceedance above wind noise (Fig. 3b) yielded a very similar distribution of noise hotspots to the maps of overall noise levels (Fig. 3a). However, it is this exceedance of natural background sound which is important to consider when assessing the

potential impact of underwater noise on marine life (Clark et al., 2009; Hatch et al., 2012), since anthropogenic noise below this level would generally be masked by the natural soundscape. This approach could be further tailored to particular species when the hearing sensitivity is known, by filtering the noise maps to reflect the audible sound above natural background (Erbe et al., 2014). By combining such pressure maps with the distribution or habitat of the target species, areas where noise management measures may have the greatest benefit can be identified (Merchant et al., 2018).

Predicted noise levels decreased with increasing frequency (Fig. 4). This was expected due to the higher source levels of ship noise at low frequencies (Wales and Heitmeyer, 2002), and poorer sound propagation at high frequencies. This also indicates that the broadband ship noise excess levels (Fig. 3) were dominated by the contribution of the 63-Hz frequency band.

Higher ship noise excess levels were observed during the summer, with the highest levels in May and July (Fig. 5c, Fig. 5d) and the lowest levels in January and November (Fig. 5a, Fig. 5f). This may be due to the summer months having both lower levels of wind noise and higher levels of shipping (possibly related to the better weather conditions), leading to a compound effect on the exceedance of ship noise above wind noise. Another variable is the degree of sound propagation loss, which varies with the sound speed profile in the water column and seabed. If propagation loss is lower, ship noise will propagate further, while wind noise is more localised due to the planar geometry of the sound source. However, sound propagation loss in a shallow water waveguide is lower in cold water, and so this effect would be expected to increase ship noise excess in winter (the temperature minimum is in March). This was not observed, indicating that this water temperature effect may be less significant than the variability in levels of shipping activity and wind noise generation. However, the sound speed profile may also have influenced this result, and we were unable to test this.

Table 1

Discrepancy between model and field measurements for median (P50) SPL for all the 1/3 octave frequency bands and validation datasets. Negative values denote underestimation in SPL by the model. A map of the monitoring locations is provided in the Supplementary Material.

Frequency (Hz)	April Site 2	April Site 3	April Site 4	May Site 2	May Site 3	May Site 4	August Site 1	August Site 2
63	1.9	-7.9	3.4	4.2	-10.8	-2.6	6.0	-6.1
80	0.8	-6.4	1.4	3.7	-8.7	-3.7	2.3	-4.3
100	0.7	-4.7	1.2	2.8	-5.8	-2.6	1.6	-3.6
125	0.8	-2.5	2.1	2.5	-2.7	-0.7	1.2	-2.5
158	0.6	-1.3	1.5	2.4	-0.7	0.2	0.4	-2.0
200	0.6	-0.6	0.8	2.0	0.3	0.8	0.0	-1.2
250	1.1	1.1	2.0	2.8	2.3	2.5	0.9	-0.2
316	0.7	1.6	2.3	2.3	3.1	2.8	1.5	-0.1
400	-1.0	1.0	1.5	0.5	2.6	1.9	1.1	-1.4
500	-1.9	0.6	1.1	-0.2	2.5	1.7	1.1	-1.8
630	-2.7	0.1	0.8	-1.2	1.9	1.2	0.9	-2.1
800	-3.9	-0.7	-0.3	-2.3	1.2	0.1	0.1	-2.6
1000	-1.9	1.4	1.1	0.6	3.1	1.6	2.0	-1.0
1250	1.7	3.6	3.5	3.6	6.2	4.1	4.0	2.9
1580	-0.8	2.9	1.9	1.5	4.7	2.6	4.6	2.3
2000	-2.2	1.6	0.6	0.4	3.2	0.9	2.2	0.8
2500	-3.2	0.3	-1.2	-0.6	2.3	-0.7	1.0	-0.2
3160	-1.8	1.4	-0.6	0.8	3.4	-0.1	1.0	0.7
4000	-1.5	0.7	-1.2	1.1	3.5	-0.6	0.6	0.6
5000	-2.4	-0.8	-2.6	0.5	1.8	-2.3	0.1	-1.0

4.2. Caveats

Although the model showed very good agreement with the data from the four field monitoring sites assessed, all of these sites were

near to the coast and in one area of the North Sea (see Fig. S1). To increase confidence in the model predictions in deeper waters and in other parts of the domain, further field measurements are needed.

The degree of agreement with the measurements suggests that sAIS-tracked ships dominated the soundscape at the sites where the model was validated, which would be consistent with a previous study in the area (Merchant et al., 2014). However, in some parts of the domain this may not be the case, and other sources may dominate, such as smaller vessels not carrying operational AIS transponders (Hermannsen et al., 2019), other anthropogenic sources, or natural processes. This would limit the accuracy of modelling based on AIS data and wind speed, although this study did not encounter such discrepancies in the available data. Other potential sources of error in the model include the accuracy of the ship and wind source models, the sound propagation model, and error in the measurements (see below).

The field monitoring data showed contamination from flow-generated noise, which is caused by turbulence around the hydrophone and does not propagate in the environment. This is likely to have been one factor which limited the agreement of the model with measurements below 125 Hz (see Supplementary Material), where the RMS errors exceeded 3 dB (up to 5.3 dB at 63 Hz) but remained substantially lower than for the initial model. Full details of RMS errors in the median predictions for all validation datasets and frequency bands are provided in the Supplementary Material (Table S2). A further issue with the field recordings was the presence of a resonance in the recordings which was clearly evident in the 1.25 kHz 1/3-octave band, and thought to be caused by standing waves within the air-filled cylindrical body of the sound recorders. This frequency band was excluded from the validation process for this reason.

While the propagation model used is relatively simple compared to more sophisticated approaches such as the parabolic equation method (Collins, 1993), this was necessary to make the mapping computationally feasible. However, this approach inevitably had some limitations. Aspects of sound propagation which could not be explicitly included in the model include the sea surface roughness, which may affect propagation at higher frequencies, and the receiver and source depths (since the model averages sound level across depth). These limitations are likely to explain some of the discrepancy between the model predictions and the measurements.

The ship source model used (Wales and Heitmeyer, 2002) is an ensemble model, which describes the source characteristics of an 'average' vessel, and does not allow for the prediction of individual ship signatures. While this model was found to be more accurate than other models (e.g. Breeding Jr et al., 1996; Ross, 1976), this approach limits the ability to model changes in individual ship signatures, for example to reflect prospective management measures to quieten certain classes of vessels (Merchant, 2019) or impose speed restrictions to reduce noise levels (MacGillivray et al., 2019). Work to develop more accurate individual-based ship noise models will be needed to assess the potential benefits of ship noise management measures with greater confidence.

4.3. Implications for monitoring and management

The results give confidence that sAIS-based modelling of underwater noise pollution from shipping are sufficiently accurate to be used in policymaking, provided they are validated with suitable field monitoring data. This is a promising result for the ongoing monitoring and modelling efforts to quantify levels of shipping noise in various regional seas. In Europe, EU-funded joint monitoring programmes for shipping noise mapping are underway, both in the North Sea (the JOMOPANS project) and the Northeast Atlantic (the JONAS project). Similar work is ongoing in Canadian waters (Aulanier et al., 2017; Erbe et al., 2012), particularly in the approaches to Vancouver harbour (Cominelli et al., 2018; Joy et al., 2019). More detailed work in future may allow more

detailed assessment of sources in uncertainty and improvements to model accuracy and precision.

On the policy front, these results support the use of noise mapping approaches in the implementation of legislation and policy designed to monitor and assess levels of anthropogenic noise pollution, such as the EU Marine Strategy Framework Directive (MSFD), the NOAA Ocean Noise Strategy, and the Canadian Ocean Protection Plan. The maps produced here will also help to inform the policymaking process in the Northeast Atlantic, through international cooperation under the OSPAR Convention.

5. Conclusion

This study demonstrates that shipping noise maps based on sAIS ship-tracking data can make valid predictions of noise levels suitable for policymaking and management. The results highlight how sound propagation characteristics of the environment affect levels of shipping noise pollution, and show that relying solely on shipping density without using acoustic modelling will not generally be effective. The maps produced here allow ship noise pollution to be incorporated into marine spatial planning, and will inform the development of international initiatives to address underwater noise pollution from shipping. Ultimately, shipping noise maps can be used to assess the risk of impact on acoustically sensitive species and to guide management decisions on ship quieting measures, ship speed restrictions, and spatiotemporal restrictions on shipping.

CRedit authorship contribution statement

Adrian Farcas: Conceptualization, Methodology, Software, Formal analysis, Writing - original draft, Writing - review & editing. **Claire F. Powell:** Formal analysis, Writing - review & editing. **Kate L. Brookes:** Writing - review & editing, Funding acquisition. **Nathan D. Merchant:** Conceptualization, Methodology, Writing - original draft, Writing - review & editing, Funding acquisition.

Acknowledgements

We thank Rebecca Faulkner and Ross Culloch for their helpful comments on the manuscript, and Lauren Bierman for assistance in sourcing the sAIS data. We also thank Ewan Edwards for overseeing data collection in the field, and Nienke van Geel for quality assurance of the field data. This study was funded by Defra, under project ME5224. The field measurements were funded by Marine Scotland Science as part of the ECOMMAS programme.

Declaration of competing interest

The authors declare that they have no known competing financial interests or personal relationships that could have appeared to influence the work reported in this paper.

Appendix A. Supplementary data

Supplementary data to this article can be found online at <https://doi.org/10.1016/j.scitotenv.2020.139509>.

References

- Andrew, R.K., Howe, B.M., Mercer, J.A., Dzieciuch, M.A., 2002. Ocean ambient sound: comparing the 1960s with the 1990s for a receiver off the California coast. *Acoust. Res. Lett. Online* 3, 65. <https://doi.org/https://doi.org/10.1121/1.1461915>.
- AQUO, 2015. *Validation of the noise footprint assessment model. Report of the EU-Funded FP7 Project AQUO: Achieve Quieter Oceans by Shipping Noise Footprint Reduction.*
- Aulanier, F., Simard, Y., Roy, N., Bandet, M., Gervaise, C., 2016. Groundtruthed probabilistic shipping noise modeling and mapping: application to blue whale habitat in the Gulf of St. Lawrence. *Proceedings of Meetings on Acoustics 4ENAL*, p. 70006.

- Aulanier, F., Simard, Y., Roy, N., Gervaise, C., Bandet, M., 2017. Effects of shipping on marine acoustic habitats in Canadian Arctic estimated via probabilistic modeling and mapping. *Mar. Pollut. Bull.* 125, 115–131. <https://doi.org/https://doi.org/10.1016/j.marpolbul.2017.08.002>.
- Bassett, C., Polagye, B., Holt, M., Thomson, J., 2012. A vessel noise budget for Admiralty Inlet, Puget Sound, Washington (USA). *J. Acoust. Soc. Am.* 132, 3706–3719. <https://doi.org/https://doi.org/10.1121/1.4763548>.
- Blair, H.B., Merchant, N.D., Friedlaender, A.S., Wiley, D.N., Parks, S.E., 2016. Evidence for ship noise impacts on humpback whale foraging behaviour. *Biol. Lett.* 12, 20160005.
- Breeding Jr., J.E., Pflug, L.A., Bradley, M., Walrod, M.H., 1996. Research Ambient Noise Directionality (RANDI) 3.1 Physics Description. Naval Research Lab Stennis Space Center MS.
- Cefas, 2015. Impacts of noise and use of propagation models to predict the recipient side of noise. Report Prepared under Contract ENV.D.2/FRA/2012/0025 for the European Commission. Centre for Environment, Fisheries & Aquaculture Science, UK.
- Clark, C.W., Ellison, W.T., Southall, B.L., Hatch, L., Van Parijs, S.M., Frankel, A., Ponirakis, D., 2009. Acoustic masking in marine ecosystems: intuitions, analysis, and implication. *Mar. Ecol. Prog. Ser.* 395, 201–222. <https://doi.org/https://doi.org/10.3354/meps08402>.
- Collins, M.D., 1993. A split-step Padé solution for the parabolic equation method. *J. Acoust. Soc. Am.* 93, 1736–1742. <https://doi.org/https://doi.org/10.1121/1.406739>.
- Cominelli, S., Devillers, R., Yurk, H., MacGillivray, A., McWhinnie, L., Canessa, R., 2018. Noise exposure from commercial shipping for the southern resident killer whale population. *Mar. Pollut. Bull.* 136, 177–200. <https://doi.org/10.1016/j.marpolbul.2018.08.050>.
- Copernicus, 2019. Copernicus Marine Environment Monitoring Service [WWW Document]. URL <http://www.ecmwf.int/en/forecasts/datasets/archive-datasets/reanalysis-datasets/era-interim>.
- Debuschere, E., Hostens, K., Adriaens, D., Ampe, B., Botteldooren, D., De Boeck, G., De Muynck, A., Sinha, A.K., Vandendriessche, S., Van Hoorbeke, L., Vincx, M., Degraer, S., 2016. Acoustic stress responses in juvenile sea bass *Dicentrarchus labrax* induced by offshore pile driving. *Environ. Pollut.* 208, 747–757. <https://doi.org/https://doi.org/10.1016/j.envpol.2015.10.055>.
- ECMWF, 2019. ERA-interim model. European Centre for Medium-Range Weather Forecasts, Reading, UK [WWW Document]. URL <http://www.ecmwf.int/en/forecasts/datasets/archive-datasets/reanalysis-datasets/era-interim>.
- Erbe, C., MacGillivray, A., Williams, R., 2012. Mapping cumulative noise from shipping to inform marine spatial planning. *J. Acoust. Soc. Am.* 132, EL423–EL428. <https://doi.org/10.1121/1.4758779>.
- Erbe, C., Williams, R., Sandilands, D., Ashe, E., 2014. Identifying modeled ship noise hotspots for marine mammals of Canada's Pacific region. *PLoS One* 9, e98920. <https://doi.org/10.1371/journal.pone.0089820>.
- European Commission, 2017. Commission decision (EU) 2017/848 of 17 May 2017 laying down criteria and methodological standards on good environmental status of marine waters and specifications and standardised methods for monitoring and assessment, and repealing decision 2010/477/EU. *Off. J. Eur. Union* 2017, 32. https://doi.org/http://eur-lex.europa.eu/pr/en/oj/dat/2003/l_285/l_28520031101en00330037.pdf.
- Farcas, A., Thompson, P.M., Merchant, N.D., 2016. Underwater noise modelling for environmental impact assessment. *Environ. Impact Assess. Rev.* 57, 114–122. <https://doi.org/10.1016/j.eiar.2015.11.012>.
- Frisk, G.V., 2012. Noiseconomics: the relationship between ambient noise levels in the sea and global economic trends. *Sci. Rep.* 2, 2–5. <https://doi.org/10.1038/srep00437>.
- Hamilton, E.L., 1987. Acoustic properties of sediments. *Acoust. Ocean Bottom* 3–58.
- Hatch, L.T., Clark, C.W., Van Parijs, S.M., Frankel, A.S., Ponirakis, D.W., 2012. Quantifying loss of acoustic communication space for right whales in and around a U.S. National Marine Sanctuary. *Conserv. Biol.* 26, 983–994. <https://doi.org/10.1111/j.1523-1739.2012.01908.x>.
- Hermanssen, L., Beedholm, K., Tougaard, J., Madsen, P.T., 2014. High frequency components of ship noise in shallow water with a discussion of implications for harbor porpoises (*Phocoena phocoena*). *J. Acoust. Soc. Am.* 136, 1640–1653. <https://doi.org/10.1121/1.4893908>.
- Hermanssen, L., Mikkelsen, L., Tougaard, J., Beedholm, K., Johnson, M., Madsen, P.T., 2019. Recreational vessels without automatic identification system (AIS) dominate anthropogenic noise contributions to a shallow water soundscape. *Sci. Rep.* <https://doi.org/10.1038/s41598-019-51222-9>.
- IMO, 2014. Guidelines for the Reduction of Underwater Noise from Commercial Shipping to Address Adverse Impacts on Marine Life. International Maritime Organisation, London, UK (IMO MEPC.1/Circ.833).
- Jansen, E., De Jong, C., 2017. Experimental assessment of underwater acoustic source levels of different ship types. *IEEE J. Ocean. Eng.* 42, 439–448. <https://doi.org/10.1109/OJE.2016.2644123>.
- Jensen, F.B., Kuperman, W.A., Porter, M.B., Schmidt, H., 2011. Computational Ocean Acoustics. Springer, NY <https://doi.org/10.1063/1.4765904>.
- Joy, R., Tollit, D., Wood, J., MacGillivray, A., Li, Z., Trounce, K., Robinson, O., 2019. Potential benefits of vessel slowdowns on endangered southern resident killer whales. *Front. Mar. Sci.* 6, 344.
- MacGillivray, A., McPherson, C., McPherson, G., Izett, J., Gosselin, J., Li, Z., Hannay, D., 2014. Modelling underwater shipping noise in the Great Barrier Reef Marine Park using AIS vessel track data. *Proceedings of Inter-Noise 2014*, p. 10.
- MacGillivray, A.O., Li, Z., Hannay, D.E., Trounce, K.B., Robinson, O.M., 2019. Slowing deep-sea commercial vessels reduces underwater radiated noise. *J. Acoust. Soc. Am.* 146, 340–351. <https://doi.org/10.1121/1.5116140>.
- McKenna, M.F., Wiggins, S.M., Hildebrand, J.A., 2013. Relationship between container ship underwater noise levels and ship design, operational and oceanographic conditions. *Sci. Rep.* 3. <https://doi.org/10.1038/srep01760>.
- McQuinn, I.H., Lesage, V., Carrier, D., Larrivière, G., Samson, Y., Chartrand, S., Michaud, R., Theriault, J., 2011. A threatened beluga (*Delphinapterus leucas*) population in the traffic lane: vessel-generated noise characteristics of the Saguenay-St. Lawrence Marine Park, Canada. *J. Acoust. Soc. Am.* 130, 3661–3673. <https://doi.org/10.1121/1.3658449>.
- Mennitt, D., Sherrill, K., Fristrup, K., 2014. A geospatial model of ambient sound pressure levels in the contiguous United States. *J. Acoust. Soc. Am.* 135, 2746–2764. <https://doi.org/10.1121/1.4870481>.
- Merchant, N.D., 2019. Underwater noise abatement: economic factors and policy options. *Environ. Sci. Pol.* 92, 116–123. <https://doi.org/10.1016/j.envsci.2018.11.014>.
- Merchant, N.D., Pirota, E., Barton, T.R., Thompson, P.M., 2014. Monitoring ship noise to assess the impact of coastal developments on marine mammals. *Mar. Pollut. Bull.* 78, 85–95. <https://doi.org/10.1016/j.marpolbul.2013.10.058>.
- Merchant, N.D., Brookes, K.L., Faulkner, R.C., Bicknell, A.W.J., Godley, B.J., Witt, M.J., 2016. Underwater noise levels in UK waters. *Sci. Rep.* 6. <https://doi.org/10.1038/srep36942>.
- Merchant, N.D., Faulkner, R.C., Martinez, R., 2018. Marine noise budgets in practice. *Conserv. Lett.* 11, e12420. <https://doi.org/10.1111/cons.12420>.
- Møhl, B., 1981. Masking effects of noise: their distribution in time and space. *The Question of Sound from Icebreaker Operations: Proceedings from a Workshop. Arctic Pilot Project, Calgary, AB*, pp. 59–66.
- Nowacek, D.P., Thorne, L.H., Johnston, D.W., Tyack, P.L., 2007. Responses of cetaceans to anthropogenic noise. *Mamm. Rev.* 37, 81–115. <https://doi.org/10.1111/j.1365-2907.2007.00104.x>.
- PAME, 2019. Underwater Noise in the Arctic: A State of Knowledge Report. Protection of the Arctic Marine Environment (PAME) Secretariat, Akureyri. <https://www.pame.is/index.php/document-library/pame-reports-new/pame-ministerial-deliverables/2019-11th-arctic-council-ministerial-meeting-rovaniemifinland/421-underwater-noise-rep>.
- Parks, S.E., Clark, C.W., Tyack, P.L., 2007. Short- and long-term changes in right whale calling behavior: the potential effects of noise on acoustic communication. *J. Acoust. Soc. Am.* 122, 3725–3731. <https://doi.org/10.1121/1.2799904>.
- Putland, R.L., Merchant, N.D., Farcas, A., Radford, C.A., 2018. Vessel noise cuts down communication space for vocalizing fish and marine mammals. *Glob. Chang. Biol.* 24, 1708–1721. <https://doi.org/10.1111/gcb.13996>.
- Reeder, D.B., Sheffield, E.S., Mach, S.M., 2011. Wind-generated ambient noise in a topographically isolated basin: a pre-industrial era proxy. *J. Acoust. Soc. Am.* 129, 64–73. <https://doi.org/10.1121/1.3514379>.
- Richardson, W.J., Würsig, B., 1997. Influences of man-made noise and other human actions on cetacean behaviour. *Mar. Freshw. Behav. Physiol.* <https://doi.org/10.1080/10236249709379006>.
- Richardson, W.J., Greene, C.R.J., Malm, C.I., Thomson, D.H., 1995. *Marine Mammals and Noise*. Academic Press.
- Rolland, R.M., Parks, S.E., Hunt, K.E., Castellote, M., Corkeron, P.J., Nowacek, D.P., Wasser, S.K., Kraus, S.D., 2012. Evidence that ship noise increases stress in right whales. *Proc. R. Soc. B Biol. Sci.* 279 (1737), 2363–2368. <https://doi.org/10.1098/rspb.2011.2429>.
- Ross, D., 1976. *Mechanics of Underwater Noise*. Pergamon.
- Sertlek, H.O., Slabbekoorn, H., ten Cate, C., Ainslie, M.A., 2019. Source specific sound mapping: spatial, temporal and spectral distribution of sound in the Dutch North Sea. *Environ. Pollut.* 247, 1143–1157. <https://doi.org/10.1016/j.envpol.2019.01.119>.
- Simard, Y., Roy, N., Gervaise, C., Giard, S., 2016. Analysis and modeling of 255 source levels of merchant ships from an acoustic observatory along St. Lawrence Seaway. *J. Acoust. Soc. Am.* 140, 2002–2018.
- Stanley, J.A., Van Parijs, S.M., Hatch, L.T., 2017. Underwater sound from vessel traffic reduces the effective communication range in Atlantic cod and haddock. *Sci. Rep.* 7. <https://doi.org/10.1038/s41598-017-14743-9>.
- Thorp, W.H., 1967. Analytic description of the low-frequency attenuation coefficient. *J. Acoust. Soc. Am.* 42, 270. <https://doi.org/10.1121/1.1910566>.
- Trigg, L.E., Chen, F., Shapiro, G.I., Ingram, S.N., Embling, C.B., 2018. An adaptive grid to improve the efficiency and accuracy of modelling underwater noise from shipping. *Mar. Pollut. Bull.* 131, 589–601. <https://doi.org/10.1016/j.marpolbul.2018.04.034>.
- UN, 2018. Nineteenth Meeting of the United Nations Open-Ended Informal Consultative Process on Oceans and the Law of the Sea: Anthropogenic Underwater Noise. 18–22 June 2018, New York.
- UNCTAD, 2017. Review of Maritime Transport 2017. United Nations Conference On Trade and Development, United Nations, Geneva, Switzerland. http://unctad.org/en/PublicationsLibrary/rmt2017_en.pdf.
- Wales, S.C., Heitmeyer, R.M., 2002. An ensemble source spectra model for merchant ship radiated noise. *J. Acoust. Soc. Am.* 111, 1211–1231. <https://doi.org/10.1121/1.1427355>.
- Weilgart, L., 2018. The Impact of Ocean Noise Pollution on Fish and Invertebrates. Report for OceanCare, Switzerland. https://www.oceancare.org/wp-content/uploads/2017/10/OceanNoise_FishInvertebrates_May2018.pdf.
- Wenz, G.M., 1962. Acoustic ambient noise in the ocean: spectra and sources. *J. Acoust. Soc. Am.* 34, 1936–1956. <https://doi.org/https://doi.org/10.1121/1.1909155>.
- Weston, D.E., 1971. Intensity-range relations in oceanographic acoustics. *J. Sound Vib.* 18, 271–287. [https://doi.org/10.1016/0022-460X\(71\)90350-6](https://doi.org/10.1016/0022-460X(71)90350-6).
- Wisniewska, D.M., Johnson, M., Teilmann, J., Siebert, U., Galatius, A., Dietz, R., Madsen, P.T., 2018. High rates of vessel noise disrupt foraging in wild harbour porpoises (*Phocoena phocoena*). *Proc. R. Soc. London B Biol. Sci.* 285. <https://doi.org/10.1098/rspb.2017.2314>.
- Wysocki, L.E., Dittami, J.P., Ladich, F., 2006. Ship noise and cortisol secretion in European freshwater fishes. *Biol. Conserv.* 128, 501–508. <https://doi.org/10.1016/j.biocon.2005.10.020>.